

# Coordinate-free Stochastic Differential Equations as Jets

John Armstrong  
Dept. of Mathematics  
King's College London  
john.1.armstrong@kcl.ac.uk

Damiano Brigo  
Dept. of Mathematics  
Imperial College London  
damiano.brigo@imperial.ac.uk

First version: October 1, 2015. This version: May 6, 2022

## Abstract

We explain how Itô Stochastic Differential Equations on manifolds may be defined as 2-jets of curves. We use jets as a natural language to express geometric properties of SDEs and show how jets can lead to intuitive representations of Itô SDEs, including three different types of drawings. We explain that the mainstream choice of Fisk-Stratonovich-McShane calculus for stochastic differential geometry is not necessary and elaborate on the relationships with the jets approach. We consider the two calculi as being simply different coordinate systems for the same underlying coordinate-free stochastic differential equation. If the extrinsic approach to differential geometry is adopted, then Stratonovich calculus may appear to be necessary when studying SDEs on submanifolds but in fact one can use the Itô/2-jets framework proposed here by recalling that the curvature of the 2-jet follows the curvature of the manifold. We argue that the choice between Itô and Stratonovich is a modelling choice dictated by the type of problem one is facing and the related desiderata. We also discuss the forward Kolmogorov equation and the backward diffusion operator in geometric terms, and consider percentiles of the solutions of the SDE and their properties, leading to fan diagrams and their relationship with jets. In particular, the median of a SDE solution is associated to the drift of the SDE in Stratonovich form for small times. Finally, we prove convergence of the 2-jet scheme to classical Itô SDEs solutions.

**Keywords:** Jets, 2-jets, stochastic differential equations, manifolds, SDEs on manifolds, stochastic differential geometry, mean square convergence, numerical schemes, Euler scheme, 2-jet scheme, SDEs drawings, Itô calculus, Stratonovich calculus, Fan Diagram, SDE median, SDE mode, SDE quantile, Forward Kolmogorov Equation, Fokker Planck Equation, 2-Jet Scheme Convergence, Coordinate-Free SDEs.

AMS classification codes: 58A20, 39A50, 58J65, 60H10, 60J60, 65D18

# 1 Introduction

This paper examines the geometry of stochastic differential equations using a coordinate free approach. Our aims are threefold:

- (i) show how to visualize stochastic differential equations (SDEs);
- (ii) show that a coordinate free formulation of stochastic differential equations on manifolds is both possible and enlightening;
- (iii) understand the geometric meaning of the coefficients of Itô and Stratonovich stochastic differential equations.

Most texts on SDEs take an extremely algebraic approach to the subject. By contrast, this paper considers the question of how to draw an SDE in a way that makes Itô's lemma intuitively clear. In particular we will illustrate a way of drawing an SDE on a rubber sheet such that if the sheet is stretched, the diagram transforms according to Itô's lemma. In other words given an SDE in  $\mathbb{R}^n$  we give a method of drawing SDEs such that for all  $f : \mathbb{R}^n \rightarrow \mathbb{R}^n$  the following diagram commutes:

$$\begin{array}{ccc}
 \text{SDE for } X & \xrightarrow{\text{Itô's lemma}} & \text{SDE for } f(X) \\
 \text{Draw} \downarrow & & \text{Draw} \downarrow \\
 \text{Picture of SDE for } X \text{ in } \mathbb{R}^n & \xrightarrow{f} & f(\text{Picture of SDE for } X)
 \end{array} \tag{1}$$

We will address this question in Section 2 in the case of an SDE driven by a single Brownian motion. We will also show how our diagrams can be interpreted in terms of a convergent discrete time numerical scheme and will prove its convergence in the more general case of a SDE driven by a vector Brownian motion. Importantly, our discrete-time scheme can be formulated in coordinate free language using the geometric notion of jets. Thus our method of drawing SDEs is general enough to make it possible to draw an SDE on a manifold and it naturally gives rise to a coordinate free method of formulating SDEs on manifolds.

It is well known that vectors on a manifold can be understood from a number of different perspectives. Firstly tangent vectors can be defined in terms of local coordinates and their transformation rules. Secondly one can define vectors in terms of operators, specifically as linear functions on the space of germs of smooth functions that also obey the Leibniz rule. A third definition of a vector is as a first order approximation to a curve on a manifold. Fourth, one can understand a vector field as an infinitesimal diffeomorphism of a manifold. Since in addition vector fields can be interpreted as ordinary differential equations (ODEs) on a manifold, this gives four ways of understanding ODEs.

In this paper we will study the parallel interpretations for SDEs. The first approach was used by Itô in [13] to define SDEs on manifolds. The second approach is coordinate free and is related to understanding SDEs in terms of

diffusion operators (see [10] for the case of  $\mathbb{R}^n$ ). The third approach corresponds to our interpretation of SDEs in terms of jets. The fourth approach corresponds to Stratonovich calculus. Many texts such as [6, 20], use Stratonovich calculus to define SDEs on manifolds. The point we wish to emphasize is that this is by no means the only way to the differential geometry of SDEs in a coordinate independent manner.

The relationship between the jet formulation and the differential operator formulation of SDEs is the topic of Section 3. We will use the language of jets to give geometric expressions for many important concepts that arise in stochastic analysis. These geometric representations are in many ways more elegant than the traditional representations in terms of the coefficients of SDEs. In particular we will give coordinate free formulations of the following: Itô's lemma; the diffusion operators; Itô SDEs on manifolds and Brownian motion on Riemannian manifolds.

Also in Section 3, we show how our definition of SDE's driven by a single Brownian motion can be generalized to processes driven by multiple Brownian motions. We show how to draw such SDE's and illustrate this using the Heston stochastic volatility model (two-dimensional diffusion) and Brownian motion on the torus.

In Section 4 we consider how our formulation is related to the Stratonovich formulation of SDEs. We will prove that sections of the bundle of  $n$ -jets of curves in a manifold correspond naturally to  $n$ -tuples of vector fields in the manifold. This generalizes the correspondence between Itô calculus and Stratonovich calculus to  $n$ -jets. This correspondence also shows that Itô calculus and Stratonovich calculus can both be interpreted as simply a choice of coordinate system for the space of sections of the bundle of  $n$ -jets of curves. Moreover, our result provides a geometric interpretation of the Itô-Stratonovich transformation, expressing the relationship between Itô and Stratonovich calculus.

In Section 5 we consider an alternative approach to drawing SDEs in one dimension. We will see that the 2-jet defining an Itô SDE can be interpreted as defining a *fan diagram* showing the limiting trajectories of certain percentiles of the probability distributions associated with the SDE solution process. Moreover we will show that the drift vector of the Stratonovich formulation can be similarly interpreted as a short-time approximation to the median. This observation is related to the coordinate independence of 2-jets and vector fields and the coordinate independence of the notion of median. By contrast the mean of a process is coordinate dependent and its short time behaviour is given by the drift vector in the Ito formulation. We will also consider short time behaviour of the mode.

We conclude by remarking that our work has numerous applications:

- (i) Differential geometry of SDEs. Coordinate free calculations in differential geometry are often simpler, shorter and more insightful than their local coordinate counterparts. As an application of our theory we were able to define a novel notion of projection for SDEs ([2, 1]). The local coordinate

formulation of the projection of an SDE is difficult to compute and it is difficult to even check that it has the correct properties under coordinate change. The coordinate free formulation by contrast is short, elegant and manifestly invariant.

- (ii) Pedagogy. For the many students who prefer to understand mathematics geometrically rather than algebraically, a diagram of an Itô SDE will be very helpful.
- (iii) Qualitative analysis of SDEs. One can gain considerable understanding of an ODE simply by drawing the corresponding vector field. The same applies to SDEs by drawing the 2-jet.

## 2 SDEs as fields of curves driven by a single Brownian motion

### 2.1 Drawing and simulating SDEs as “fields of curves”

Suppose that at every point  $x$  in  $\mathbb{R}^n$  we have an associated smooth curve:

$$\gamma_x : \mathbb{R} \rightarrow \mathbb{R}^n \quad \text{with } \gamma_x(0) = x$$

As an example we might define  $\gamma_x^E$  on  $\mathbb{R}^2$  as follows:

$$\gamma_{(x_1, x_2)}^E(t) = (x_1, x_2) + t(-x_2, x_1) + 3t^2(x_1, x_2)$$

This specific case is chosen for a number of reasons. We have a radially outward  $t^2$  component and an orthogonal counterclockwise circular component  $t$ . This allows us to draw a good picture of the trajectories and also to lead to a good transformation when using polar coordinates. This specific example has zero derivatives with respect to  $t$  from the third derivative on. We stop at second order in  $t$  since this will be enough to converge to classical stochastic calculus, as we will see. However, one should also check that for well behaved curves, higher order terms would not lead to limits that are different from the limit obtained from terms up to order two. Indeed, further on in this paper we will consider also more general  $\gamma_x$  curves with nonzero higher order derivatives, and we will show that under some assumptions on the third derivatives of  $t \mapsto \gamma_x(t)$ , only the first and second order terms contribute to form the limits converging to classical stochastic calculus, and we may ignore terms of order higher than two.

We will use the superscript  $E$  to indicate this example process throughout. We have plotted  $\gamma^E$  in figure 1.

To be precise we have taken a grid of points in  $\mathbb{R}^2$  which are marked as dots in the figure. We have then drawn the curve  $\gamma_x^E$  at each grid point  $x$  for the parameter values  $t$  in  $(-0.1, 0.1)$ . In general when drawing such a figure for a general  $\gamma$ , one should use the same range  $t \in (-\epsilon, \epsilon)$  for every curve in the figure, but one is free to choose  $\epsilon$  to make the diagram visually appealing. (In

just the same way when drawing vector fields, one chooses a sensible scale for each vector).

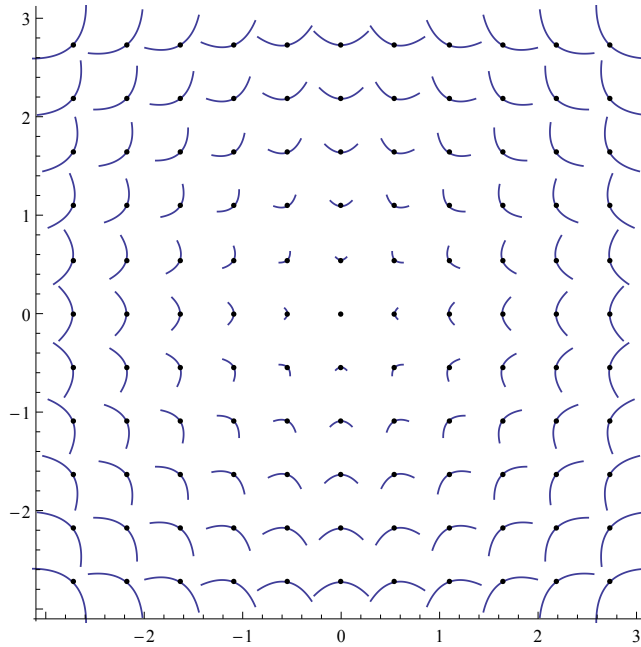


Figure 1: A plot of  $\gamma^E$

Given such a  $\gamma$ , a starting point  $x_0$  (the deterministic origin in our example,  $X_0 = 0$ ), a Brownian motion  $W_t$  and a time step  $\delta t$  we can define a discrete time stochastic process using the following recurrence relation:

$$X_0 := x_0, \quad X_{t+\delta t} := \gamma_{X_t}(W_{t+\delta t} - W_t) \quad (2)$$

In Figure 2 we have plotted the trajectories of process for  $\gamma^E$ , the starting point  $(1, 0)$ , a fixed realization of Brownian motion and a number of different time steps. Rather than just plotting a discrete set of points for this discrete time process, we have connected the points using the curves in  $\gamma_{X_t}^E$ .

Notice that since the  $\delta W_t = W_{t+\delta t} - W_t$  are normally distributed with standard deviation  $\sqrt{\delta t}$  we can interpret the trajectories as being randomly generated trajectories that move from  $X_t$  to  $X_{t+\delta t}$  by following the curve  $s \mapsto \gamma_{X_t}(s)$  from  $s = 0$  to  $s = \epsilon_t \sqrt{\delta t}$  where the  $\epsilon_t$  are independent normally distributed random variables.

As the figure suggests, these discrete time stochastic processes (2) converge in some sense to a limit as the time step tends to zero.

We will use the following notation for the limiting process:

$$\text{Coordinate free SDE: } X_t \curvearrowright \gamma_{X_t}(dW_t), \quad X_0 = x_0. \quad (3)$$

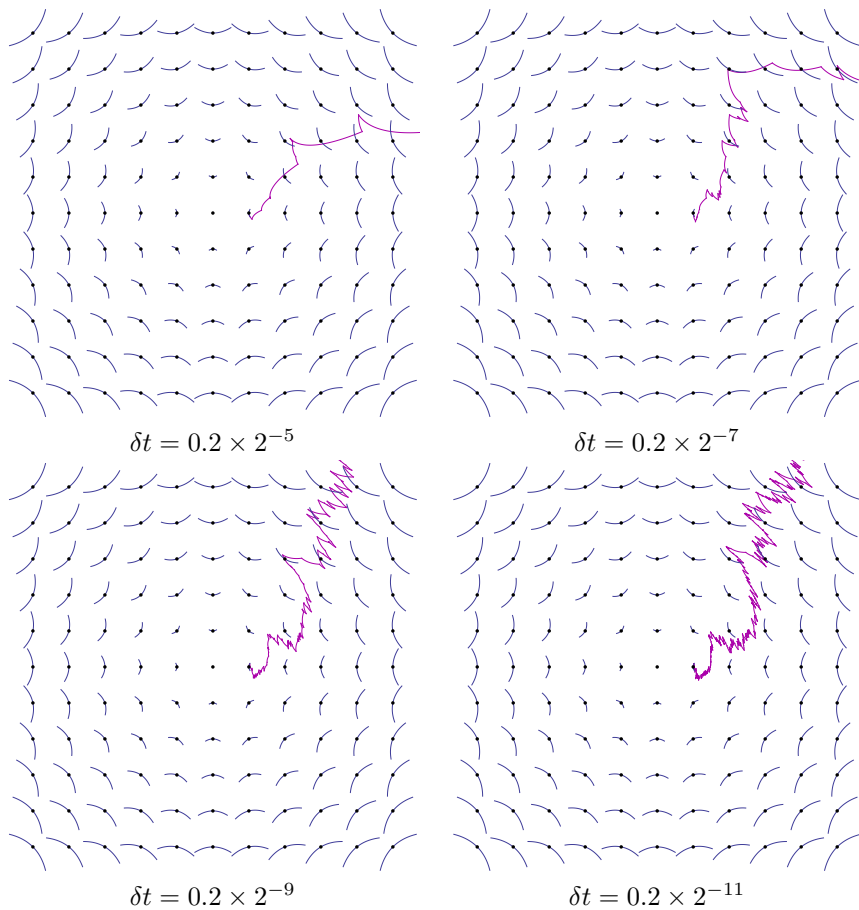


Figure 2: Discrete time trajectories for  $\gamma^E$  for a fixed  $W_t$  and  $X_0$  with different values for  $\delta t$

For the time being, let us simply treat equation (3) as a short-hand way of saying that equation (2) converges in some sense to a limit. Note that it will not converge for arbitrary  $\gamma$ 's but it does converge for nice  $\gamma$  such as  $\gamma^E$  or  $\gamma$ 's with sufficiently good regularity. The reader familiar with Itô calculus will want to know how this notation corresponds to Itô stochastic differential equations and in precisely what sense and under what circumstances equation (2) converges to a limit. These questions are addressed in Section. 2.2.

An important feature of equation (2) is that it makes no reference to the vector space structure of  $\mathbb{R}^n$  for our state space  $X$ . We have maintained this in the formal notation used in equation (3). By avoiding using the vector space structure on  $\mathbb{R}^n$  we will be able to obtain a coordinate free understanding of stochastic differential equations.

**Example 1.** For a fixed  $\alpha \in \mathbb{N}$  we can define curves at each point in  $\mathbb{R}$  by:

$$\gamma_x^\alpha(s) = x + s^\alpha$$

Let us compute the limit of the discrete time process corresponding to these curves. In the case  $\alpha = 1$ , we have trivially that the  $X_t = x_0 + W_t$ . By equation (2) we have that:

$$\begin{aligned} X_{n\delta t} &= x_0 + \sum_{i=1}^n (W_{(i+1)\delta t} - W_{i\delta t})^\alpha \\ &= x_0 + (\delta t)^{\frac{\alpha}{2}} \sum_{i=1}^n \epsilon_i^\alpha \end{aligned}$$

where the  $\epsilon_i$  are independently normally distributed with mean 0 and standard deviation 1. Fixing a terminal time  $T$  so that  $\delta t = \frac{T}{n}$  we have:

$$X_T = x_0 + (T/n)^{\frac{\alpha}{2}} \sum_{i=1}^n \epsilon_i^\alpha.$$

By the central limit theorem we see that if  $\alpha = 2$  this converges in distribution to a Dirac mass centered on  $x_0 + T$ . If  $\alpha \geq 3$  we see that this converges to a Dirac mass centered on  $x_0$ .

## 2.2 SDEs as fields of curves up to order 2: 2-jets

Let us now invoke explicitly the  $\mathbb{R}^n$  structure of the state space and consider the (component-wise) Taylor expansion of  $\gamma_x$ . We have:

$$\gamma_x(t) = x + \gamma'_x(0)t + \frac{1}{2}\gamma''_x(0)t^2 + R_x t^3, \quad R_x = \frac{1}{6}\gamma'''_x(\xi), \quad \xi \in [0, t],$$

where  $R_x t^3$  is the remainder term in Lagrange form. Substituting this Taylor expansion in our Equation (2) we obtain

$$\delta X_t = \gamma'_{X_t}(0)\delta W_t + \frac{1}{2}\gamma''_{X_t}(0)(\delta W_t)^2 + R_{X_t}(\delta W_t)^3, \quad X_0 = x_0. \quad (4)$$

Example 1 suggests that we can replace the term  $(\delta W_t)^2$  with  $\delta t$  and we can ignore terms of order  $(\delta W_t)^3$  and above. So we expect that under reasonable conditions the recurrence relation given by (2) will converge to the same limit as the numerical scheme:

$$\delta \bar{X}_t = \gamma'_{\bar{X}_t}(0)\delta W_t + \frac{1}{2}\gamma''_{\bar{X}_t}(0)\delta t, \quad \bar{X}_0 = x_0.$$

Defining  $a(X) := \gamma''_X(0)/2$  and  $b(X) := \gamma'_X(0)$  we have that this last equation can be written as

$$\delta \bar{X}_t = a(\bar{X}_t)\delta t + b(\bar{X}_t)\delta W_t. \quad (5)$$

It is well known that this last scheme (Euler scheme) does converge in some appropriate sense to a limit ([14]) and that this limit is given by the solution to the Itô stochastic differential equation:

$$d\tilde{X}_t = a(\tilde{X}_t) dt + b(\tilde{X}_t) dW_t, \quad \tilde{X}_0 = x_0. \quad (6)$$

Thus we may think of equation (2) as defining a numerical scheme for approximating the Ito SDE (6). In this context we call (2) the 2-jet scheme. A rigorous proof of the convergence of the 2-jet scheme in mean square ( $L^2(\mathbb{P})$ ) to the solution of the Ito SDE, based on appropriate bounds on the derivatives of the curves  $\gamma_x$ , is given in Appendix A.

It is important to note that the coefficients of equation (6) only depend upon the first two derivatives of  $\gamma$ . We say that two smooth curves  $\gamma : \mathbb{R} \rightarrow \mathbb{R}^n$  have the same  $n$ -jet if they are equal up to order  $O(t^n)$ . Using this terminology, we say that the coefficients of equation (6) (and (5)) are determined by the 2-jet of a curve  $\gamma : \mathbb{R} \rightarrow \mathbb{R}^n$ .

Jets are defined in much more general terms in differential geometry, for example they can be defined as equivalence classes of maps with the same Taylor expansion up to a given order. They represent abstract Taylor expansions that allow one to approach differential equations on manifolds in a coordinate-free manner. Also, jets and the related notions of obstruction and symbol are powerful tools in the analysis of differential equations in a geometric setting.

In the light of this result, we can say that in pictures such as Figure 1 one should avoid interpreting any details other than the first two derivatives of the curve. One way of doing this is by insisting that we draw the quadratic curves that best fit the curves  $\gamma$  rather than the actual curve  $\gamma$  itself.

Notice that vectors can be defined in the same way as 1-jets of smooth curves. In just the same way as we draw quadratic curves in Figure 1, one normally chooses to draw straight lines in a diagram of a vector field.

In summary: vector fields are fields of 1-jets and they represent ODE's; diagrams such as Figure 1 are pictures of fields of 2-jets and they represent Itô SDEs.

Given a curve  $\gamma_x$ , we will write  $j_2(\gamma_x)$  for the two jet associated with  $\gamma_x$ . This is formally defined to be the equivalence class of all curves which are equal to  $\gamma_x$  up to  $O(t^3)$ .

Since we will show that, under reasonable regularity conditions, the limit of the symbolic equation (3) depends only on the 2-jet of the driving curve, we may rewrite equation (3) as:

$$\text{Coordinate-free 2-jet SDE:} \quad X_t \rightsquigarrow j_2(\gamma_{X_t})(dW_t), \quad X_0 = x_0. \quad (7)$$

This may be interpreted either as a coordinate free notation for the classical Itô SDE given by equation (6) or as a shorthand notation for the limit of the process given by the discrete time equation (2).

### 2.3 Coordinate-free Itô formula with jets

Suppose that  $f$  is a smooth mapping from  $\mathbb{R}^n$  to itself and suppose that  $X$  satisfies (2). It follows that  $f(X)$  satisfies:

$$(f(X))_{t+\delta t} = f \circ \gamma_{X_t}(\delta W_t).$$

Taking the limit as  $\delta t$  tends to zero we have:

**Lemma 1.** *[Itô's lemma — coordinate free formulation] If the process  $X_t$  satisfies*

$$X_t \rightsquigarrow j_2(\gamma_{X_t})(dW_t)$$

then  $f(X_t)$  satisfies

$$f(X_t) \rightsquigarrow j_2(f \circ \gamma_{X_t})(dW_t)$$

If one prefers the more traditional format for SDEs given in (6) we simply need to calculate the derivatives of  $f \circ \gamma$ . Let us write  $\gamma_X^i$  for the  $i$ -th component of  $\gamma_X$  with respect to the coordinates  $x_1, x_2, \dots, x_n$  for  $\mathbb{R}^n$ . Two applications of the chain rule give us:

$$\begin{aligned} (f \circ \gamma_X)'(t) &= \sum_{i=1}^n \frac{\partial f}{\partial x_i}(\gamma_X(t)) \frac{d\gamma_X}{dt} \\ (f \circ \gamma_X)''(t) &= \sum_{j=1}^n \sum_{i=1}^n \frac{\partial^2 f}{\partial x_i \partial x_j}(\gamma_X(t)) \frac{d\gamma_X^i}{dt} \frac{d\gamma_X^j}{dt} \\ &\quad + \sum_{i=1}^n \frac{\partial f}{\partial x_i}(\gamma_X(t)) \frac{d^2 \gamma_X}{dt^2} \end{aligned}$$

We conclude that our lemma is equivalent to the classical Itô's lemma.

*We can now interpret Itô's lemma geometrically as the statement that the transformation rule for jets under a change of coordinates is given by composition of functions.*

Since we now understand the geometric content of Itô's lemma, we can draw a picture to illustrate it. Consider the transformation  $\phi : \mathbb{R}^2/\{0\} \rightarrow [-\pi, \pi] \times \mathbb{R}$  by

$$(\theta, s) = \phi(x_1, x_2) = \left( \arctan(x_2/x_1), \log(\sqrt{x_1^2 + x_2^2}) \right),$$

or equivalently

$$\phi(\exp(s) \cos(\theta), \exp(s) \sin(\theta)) = (\theta, s),$$

applied to our example process  $\gamma^E$ . This can be viewed as a transformation of the complex plane  $\phi(z) = i \log(z)$ . We use  $\phi$  to transform the fourth picture in Figure 2 in two different ways. Firstly we apply directly  $\phi$  to each point of Figure 2 to obtain a new point to be inserted in a new figure. This is done by using image manipulation software. In other words we stretch the image without any consideration of its mathematical structure. The result of this is shown in the upper part of Figure 3.

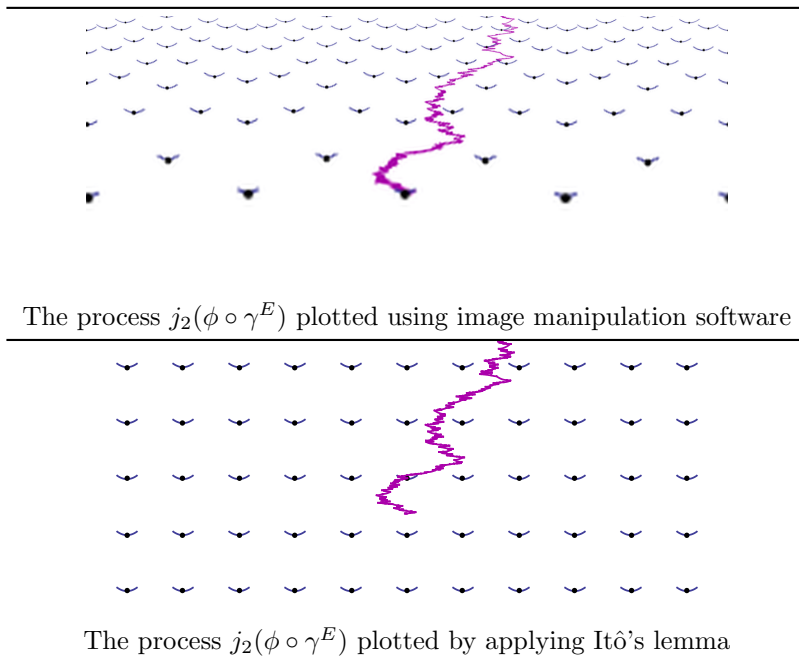


Figure 3: Two plots of the process  $j_2(\phi \circ \gamma^E)$  in the plane  $(\theta, s)$ .

As an alternative approach, we transform our equation using Itô's lemma applied to the function  $\phi$ . This results in the equation for  $\theta$  and  $s$ :

$$d(\theta, s) = \left(0, \frac{7}{2}\right) dt + (1, 0) dW_t.$$

We can then use this equation to plot the process  $(\theta, s)$  directly by simulating the process in discrete time as before. The result is shown in the lower part of Figure 3.

As one can see the two approaches to plotting the transformed process give essentially identical results, showing an example of our earlier diagram (1) at work. The differences one can see are: the lower quality in the upper image, obtained by transforming pixels rather than using vector graphics; the grid points at which the 2-jets are plotted are changed; small differences in the simulated path since we have only simulated discrete time paths.

We have assumed in our presentation so far that the 2-jet  $j_2(\gamma_x)$  is associated in a deterministic and time independent manner with the point  $x$ . However, the theory can be generalized to time dependent and stochastic choices of 2-jets.

### 3 Differential Geometry of Itô SDEs

We can now define an Itô SDE on a manifold,  $M$ , driven by a single Brownian motion  $W$  by choosing a 2-jet corresponding to the curve  $\gamma_x$  at each point  $x$  in the manifold with  $\gamma_x(0) = x$ . Our aim in this section is to show that this perspective allows one to give coordinate free definitions of the key concepts in stochastic differential geometry.

As we have already observed our discrete time formulation (equation (2)) of Itô SDEs on manifolds is already coordinate free in that it makes no mention of the vector space structure of  $\mathbb{R}^n$ . Given a field of 2-jets of curves at each point of a manifold  $M$  we can write down a corresponding Itô SDE using the notation of equation (7). This may be interpreted either as indicating the limit of the discrete time process or as a short-hand for a classical Itô SDE. The reformulation of Itô's lemma in the language of jets shows that this second interpretation will be independent of the choice of coordinates. The only issue one needs to consider are the bounds needed to ensure existence of solutions. The details of transferring the theory of existence and uniqueness of solutions of SDEs to manifolds are considered in, for example, [6], [13] and [7].

The point we wish to emphasize is that the coordinate free formulation of an SDE given in equation (7) can be interpreted just as easily on a manifold as on  $\mathbb{R}^n$ . This leads us to the following

**Definition 1. (Coordinate free Itô SDEs driven by 1-dimensional Brownian motion).** A Ito SDE on the manifold  $M$  is a section of the bundle of 2-jets of curves over  $M$  together with a one-dimensional Brownian motion  $W$ .

Let us see how this simplifies the study of the differential geometry of SDEs.

Suppose now that  $f$  is a function mapping  $M$  to  $\mathbb{R}$ . We can define a differential operator acting on *functions* in terms of a 2-jet associated with  $\gamma_x$  as follows.

**Definition 2. (Backwards diffusion operator via 2-jets).** The Backwards diffusion operator for the Itô SDE defined by the 2-jet associated with the curve  $\gamma_x$  is defined on suitable functions  $f$  as

$$\mathcal{L}_{\gamma_x}(f) := \frac{1}{2}(f \circ \gamma_x)''(0).$$

In contexts where the SDE is understood we will simply write  $\mathcal{L}$ .

Note that this definition is simply the drift term of the Itô SDE for  $f(X)$  computed using Itô's lemma. To first order, the drift measures how the expectation of a variable changes over time. Thus, with  $\delta$  denoting the forward  $t$  increment as usual:

$$(\delta\mathbb{E}[f(X_t)|X_s = x])|_{s=t} = (\mathcal{L}_{\gamma_x}(f))\delta t + O(\delta t^2) \quad (8)$$

Before proceeding to define the forward diffusion operator, let us briefly recall the theory of the bundle of densities on a manifold.

Recall that given a vector space  $V$  and a group homomorphism:

$$\tau : GL(n, \mathbb{R}) \rightarrow \text{Aut}(V)$$

we can define an associated bundle  $\mathbf{V}$  over  $M$ . The fibres of the bundle over a point  $p$  are given by equivalence classes of charts  $\phi : M \rightarrow \mathbb{R}^n$  and vectors  $v \in V$  under the relation:

$$(\phi_1, v_1) \sim (\phi_2, v_2) \iff \tau((\phi_1)_* \circ (\phi_2)_*^{-1})_p(v_2) = v_1.$$

Each chart  $\phi : M \rightarrow \mathbb{R}^n$  defines local coordinates on  $\mathbf{V}$ . We use this to define the smooth structure on  $\mathbf{V}$ . This generalizes straightforwardly [16] to allow one to associate a vector bundle with any principal  $G$ -bundle and a representation of the Lie group  $G$ . In our special case, the principal  $G$ -bundle we are using is the frame bundle of the manifold.

Now consider the representation:

$$\tau(g) = |\det(g)| \in \text{Aut}(\mathbb{R}).$$

This defines a bundle over a manifold  $M$  called the bundle of densities. This bundle is denoted  $\text{Vol}$ . The usual transformation formula for probability densities under changes of coordinates tells us that a probability density over  $M$  is a section of  $\text{Vol}$ .

Integration defines a pairing between functions and densities on  $M$  by:

$$\int : \Gamma(\mathbb{R}) \times \Gamma(\text{Vol}) \rightarrow \mathbb{R}$$

by  $\int(f, \rho) := \int f \rho.$

On non-compact manifolds one must either insist that one of  $f$  or  $\rho$  is compactly supported or consider decay rates of  $f$  and  $\rho$  to ensure this is well defined.

Note that from a probabilistic point of view, this pairing is interpreted as taking expectations.

Using integration by parts, we can define  $\mathcal{L}^*$  to be the formal adjoint of  $\mathcal{L}$  with respect to this pairing. This is called the *forward diffusion operator*.

Even if one does not know the initial state  $X_0$  but knows its probability density,  $\rho$ , one may integrate equation (8) to obtain:

$$\frac{\partial}{\partial t} \int_M f(\rho) = \int_M (\mathcal{L}f)(\rho)$$

Since this holds for all smooth compactly supported functions  $f$  we can deduce:

$$\frac{\partial \rho}{\partial t} = \mathcal{L}^*(\rho).$$

We conclude that the Fokker–Planck equation follows from Itô’s lemma for functions.

Notice that both  $\mathcal{L}$  and  $\mathcal{L}^*$  are linear second order operators. The key difference is that they have different domains.  $\mathcal{L}$  acts on functions;  $\mathcal{L}^*$  acts on densities. This gives a geometric explanation as to why  $\mathcal{L}$  appears in the Feynman–Kac equation which tells us about the evolution of expectations of functions whereas  $\mathcal{L}^*$  appears in the Fokker–Planck equation which tells us about the evolution of probability densities.

Notice also that our definitions of the diffusion operators are coordinate free.

Our discussion can be generalized to SDEs driven by  $d$  independent Brownian motions  $W_t^\alpha$  with  $\alpha \in \{1, 2, \dots, d\}$ .

**Definition 3. (SDEs in  $\mathbb{R}^n$  driven by vector-Brownian motion as 2-jets).** Consider jets of functions of the form:

$$\gamma_x : \mathbb{R}^d \rightarrow \mathbb{R}^n$$

Just as before we can consider difference equations of the form:

$$X_{t+\delta t} := \gamma_{X_t} (\delta W_t^1, \dots, \delta W_t^d)$$

or, if writing  $\delta W_t^\alpha = \epsilon_\alpha \sqrt{\delta t}$ , with  $\epsilon$  independent normals,

$$X_{t+\delta t} := \gamma_{X_t} (\epsilon_1 \sqrt{\delta t}, \dots, \epsilon_d \sqrt{\delta t}).$$

Again, the limiting behaviour of such difference equations will only depend upon the 2-jet  $j_2(\gamma_x)$  and can be denoted by (7), where it is now understood that  $dW_t$  is the vector Brownian motion increment. We can state the following theorem, showing that the 2-jet scheme converges in  $L^2(\mathbb{P})$  to the classic Itô SDE with the same coefficients in a given coordinate system. This theorem proves one of the main results of this paper: a Itô SDE can be represented in a coordinate free manner simply as a 2-jet driven by Brownian motion.

**Theorem 1. Convergence of the 2-jet schemes to Itô SDEs.** *Let  $\gamma_x : \mathbb{R}^d \rightarrow \mathbb{R}^n$  be a smoothly varying family of functions whose first and second derivatives in  $\mathbb{R}^d$  satisfy Lipschitz conditions (and hence linear growth bounds). In other words we require that there exists a positive constant  $K$  such that for all  $x, y \in \mathbb{R}^n$  and  $\alpha, \beta \in \{1, 2, \dots, d\}$  we have:*

$$\begin{aligned} & \left| \frac{\partial \gamma_x}{\partial u^\alpha} \Big|_{u=0} - \frac{\partial \gamma_y}{\partial u^\alpha} \Big|_{u=0} \right| \leq K|x - y| \\ & \left| \frac{\partial^2 \gamma_x}{\partial u^\alpha \partial u^\beta} \Big|_{u=0} - \frac{\partial^2 \gamma_y}{\partial u^\alpha \partial u^\beta} \Big|_{u=0} \right| \leq K|x - y| \\ & \left( \text{and hence } \left| \frac{\partial \gamma_x}{\partial u^\alpha} \Big|_{u=0} \right|^2 \leq K^2 (1 + |x|^2) \right. \\ & \quad \left. \left| \frac{\partial \gamma_x}{\partial u^\alpha \partial u^\beta} \Big|_{u=0} \right|^2 \leq K^2 (1 + |x|^2) \right). \end{aligned}$$

Note that we are using the letter  $u$  to denote the coordinates for  $\mathbb{R}^d$ . Suppose in addition that we have a uniform bound on the third derivatives:

$$\left| \frac{\partial^3 \gamma_x}{\partial u^\alpha \partial u^\beta \partial u^\gamma} \Big|_{u=0} \right| \leq K$$

Let  $T$  be a fixed time and let  $\mathcal{T}^N := \{0, \delta t, 2\delta t, \dots, N\delta t = T\}$ , be a set of discrete time points. Let  $X_t$  denote the 2-jet scheme defined by:

$$X_{t+\epsilon} = \gamma_{X_t}(W_{t+\epsilon} - W_t), \quad t \in \mathcal{T}^N, \quad \epsilon \in [0, \delta t], \quad X_0 = x_0, \quad (9)$$

then this converges in  $L^2(\mathbb{P})$  to the classical Itô solution of the corresponding SDE, namely

$$\tilde{X}_t = \tilde{X}_0 + \int_0^t a(\tilde{X}_s) ds + \sum_{\alpha=1}^d \int_0^t b_\alpha(\tilde{X}_s) dW_s^\alpha, \quad t \in [0, T]$$

where

$$a(x) := \frac{1}{2} \sum_{\alpha=1}^d \frac{\partial^2 \gamma_x}{\partial u^\alpha \partial u^\alpha} \Big|_{u=0}$$

and

$$b_\alpha(x) := \frac{\partial \gamma_x}{\partial u^\alpha} \Big|_{u=0}.$$

More precisely we have the estimate:

$$\sup_{t \in [0, T]} E \left\{ |X_t^N - \tilde{X}_t|^2 \right\} \leq C \delta t = C \frac{T}{N} \quad (10)$$

for some constant  $C$  independent of  $N$ . We denote the coordinate free equation obtained as limit of (9) by

$$X_t \rightsquigarrow j_2(\gamma_{X_t})(dW_t).$$

The proof is given in the appendix.

Thus the limiting SDE associated with our difference equation is:

$$dX_t = \frac{1}{2} \sum_{\alpha} \sum_{\beta} \frac{\partial^2 \gamma_{X_t}}{\partial x^\alpha \partial x^\beta} dW_t^\alpha dW_t^\beta + \sum_{\alpha} \frac{\partial \gamma_{X_t}}{\partial x^\alpha} dW_t^\alpha \quad (11)$$

Here  $x^\alpha$  are the standard orthonormal coordinates for  $\mathbb{R}^d$ . Again our equation should be interpreted with the convention that  $dW_t^\alpha dW_t^\beta = g_E^{\alpha\beta} dt$  where  $g_E$  is equal to 1 if  $\alpha$  equals  $\beta$  and 0 otherwise.

Notice that in the above definition we choose to write  $g_E$  instead of using a Kronecker  $\delta$  because one might want to choose non orthonormal coordinates for  $\mathbb{R}^d$  and so it is useful to notice that  $g_E$  represents the symmetric 2-form defining

the Euclidean metric on  $\mathbb{R}^d$ . Using as Kronecker  $\delta$  would incorrectly suggest that this term transforms as an endomorphism rather than as a symmetric 2-form. An advantage of our notation is that we can use the Einstein summation convention. For example equation (11) can then be simplified to:

$$\begin{aligned} dX_t^i &= \frac{1}{2} \partial_\alpha \partial_\beta \gamma^i dW_t^\alpha dW_t^\beta + \partial_\alpha \gamma^i dW_t^\alpha \\ &= \frac{1}{2} \partial_\alpha \partial_\beta \gamma^i g_E^{\alpha\beta} dt + \partial_\alpha \gamma^i dW_t^\alpha \end{aligned} \quad (12)$$

In the  $n$ -dimensional case we define the backward diffusion operator by:

$$\mathcal{L}_{\gamma_x} f := \frac{1}{2} \Delta_E (f \circ \gamma_x) = \frac{1}{2} \partial_\alpha \partial_\beta (f \circ \gamma_x) g_E^{\alpha\beta}. \quad (13)$$

Here  $\Delta_E$  is the Laplacian defined on  $\mathbb{R}^d$ .  $\mathcal{L}_{\gamma_x}$  acts on functions defined on  $M$ . We define  $\mathcal{L}^*$  to be its formal adjoint which acts on densities defined on  $M$ .

Again inspired by the  $\mathbb{R}^n$  case, we may state the following

**Definition 4. (Coordinate free Itô SDEs driven by vector Brownian motion).** A Ito SDE on a manifold  $M$  is a section of the bundle of 2-jets of maps  $\mathbb{R}^d \rightarrow M$  together with  $d$  Brownian motions  $W_t^i$ ,  $i = 1, \dots, d$ .

### 3.1 Weak and strong equivalence

We see that both the Itô SDE (12) and the backward diffusion operator use only part of the information contained in the 2-jet. Specifically only the diagonal terms of  $\partial_\alpha \partial_\beta \gamma^i$  (those with  $\alpha = \beta$ ) influence the SDE and even for these terms it is only their average value that is important. The same consideration applies to the backward diffusion operator. This motivates the following

**Definition 5.** We say that two 2-jets  $\gamma_x^1$  and  $\gamma_x^2$

$$\gamma_x^i : \mathbb{R} \rightarrow M$$

are *weakly equivalent* if

$$\mathcal{L}_{\gamma_x^1} = \mathcal{L}_{\gamma_x^2}.$$

We say that  $\gamma^1$  and  $\gamma^2$  are *strongly equivalent* if in addition

$$j_1(\gamma_1) = j_1(\gamma_2).$$

We see that the SDEs defined by the two sets of 2-jets are equivalent if the 2-jets are strongly equivalent. This means that given the same realization of the driving Brownian motions  $W_t^\alpha$  the solutions of the SDEs will be almost surely the same (under reasonable assumptions to ensure pathwise uniqueness of solutions to the SDEs).

When the 2-jets are weakly equivalent, the transition probability distributions resulting from the dynamics of the related SDEs are the same even though

the dynamics may be different for any specific realisation of the Brownian motions. For this reason one can define a diffusion process on a manifold as a smooth selection of a second order linear operator  $\mathcal{L}$  at each point that determines the transition of densities. A diffusion can be realised locally as an SDE, but not necessarily globally.

Recall that the top order term of a quasi linear differential operator is called its symbol. In the case of a second order quasi linear differential operator  $D$  which maps  $\mathbb{R}$ -valued functions to  $\mathbb{R}$ -valued functions, the symbol defines a section of  $S^2T$ , the bundle of symmetric tensor products of tangent vectors, which we will call  $g_D$ .

In local coordinates, if the top order term of  $D$  is:

$$Df = a^{ij} \partial_i \partial_j f + \text{lower order}$$

then  $g_D$  is given by:

$$g_D(X_i, X_j) = a^{ij} X_i X_j$$

We are using the letter  $g$  to denote the symbol for a second order operator because, in the event that  $g$  is positive definite and  $d = \dim M$ ,  $g$  defines a Riemannian metric on  $M$ . In these circumstances we will say that the SDE/diffusion is *non-singular*. Thus we can associate a canonical Riemannian metric  $g_{\mathcal{L}}$  to any non-singular SDE/diffusion.

**Definition 6.** A non-singular diffusion on a manifold  $M$  is called a Riemannian Brownian motion if

$$\mathcal{L}(f) = \frac{1}{2} \Delta_{g_{\mathcal{L}}}(f).$$

Note that given a Riemannian metric  $h$  on  $M$  there is a unique Riemannian Brownian motion (up to diffusion equivalence) with  $g_{\mathcal{L}} = h$ . This is easily checked with a coordinate calculation.

This completes our definitions of the key concepts in stochastic differential geometry and indicates some of the important connections between stochastic differential equations, Riemannian manifolds, second order linear elliptic operators and harmonic maps.

We emphasize that all our definitions are coordinate free and we have worked exclusively with Itô calculus. It is more conventional to perform stochastic differential geometry using Stratonovich calculus. The justification usually given for this is that Stratonovich calculus obeys the usual chain rule so the coefficients of Stratonovich SDEs can be interpreted as vector fields. For example one can immediately see if the trajectories to a Stratonovich SDE almost surely lie on particular submanifold by testing if the coefficients of the SDE are all tangent to the manifold. We would argue that the corresponding test for Itô SDEs is also perfectly simple and intuitive: one checks whether the 2-jets follow the curvature of the manifold. As is well known, the probabilistic properties of the Stratonovich integral are not as nice as the properties of the Itô integral. In particular the Itô integral is a martingale whereas the Stratonovich integral is not. Thus the use of Stratonovich calculus on manifolds comes at a price.

### 3.2 Drawing SDEs driven by multi-dimensional Brownian motion

We now understand that we can draw an Itô SDE driven by  $d$ -dimensional Brownian motion by drawing a function:

$$\gamma_x : \mathbb{R}^d \rightarrow M$$

at every point on the manifold  $M$ . Of course, in practice one only draws the function at a finite set of sample points in  $M$ .

To draw a function in a sensible way, one draws the image of the  $\epsilon$ -ball at each point for some chosen  $\epsilon$ . One should choose a consistent value for every sample point. The image of a function does not completely define the function, one might also want to draw labelled grid lines on the image in order to show how the coordinate system on  $\mathbb{R}^d$  is mapped to the coordinate system on the image. However, if one is only interested in SDEs up to diffusion equivalence and one's SDEs are non-singular then it is easy to check that one can recover the diffusion equivalence class of  $\gamma_x$  from just the image of the  $\epsilon$ -ball and the image of the origin.

Such a drawing is sufficient to encode the SDE, but it actually contains some redundant information about  $\gamma_x$  beyond just the diffusion equivalence class. For this reason, it is best to draw a representative of the diffusion equivalence class  $\gamma_x$  for which the matrix  $\partial_\alpha \partial_\beta \gamma_x$  is equal to  $(g_E)_{\alpha\beta}$  (here we have simply used the metric  $g_E$  to lower the indices of  $(g_E)^{\alpha\beta}$ ).

With these conventions understood, in Figure 4 we show a plot of the Heston stochastic volatility model with drift (see [12]):

$$\begin{aligned} dS_t &= \mu S_t dt + \sqrt{\nu_t} S_t dW_t^1 \\ d\nu_t &= \kappa(\theta - \nu_t) dt + \xi \sqrt{\nu_t} (\rho dW_t^1 + \sqrt{1 - \rho^2} dW_t^2) \end{aligned} \tag{14}$$

The drift term in (14) can be seen visually by the fact that the dots showing the points for which we have plotted the 2-jets are off centre in each ellipse. The metric induced by the Heston equation is shown visually by the ellipses themselves. The length of a vector starting at the centre of each ellipse and going to the boundary of the ellipse is approximately equal to  $\epsilon$  and this approximation becomes increasingly accurate as  $\epsilon$  tends to zero.

In Figure 5 we plot the corresponding figure for Riemannian Brownian motion on a torus with respect to the metric induced on the torus by the Euclidean metric on  $\mathbb{R}^3$ . As one can see, all the ellipses appear to be the same size and the points appear to be in the centre of each ellipse. This first point shows that the metric induced by Riemannian Brownian motion is indeed equal to the metric induced by the embedding. The second point shows that the forward and backward operators are equal.

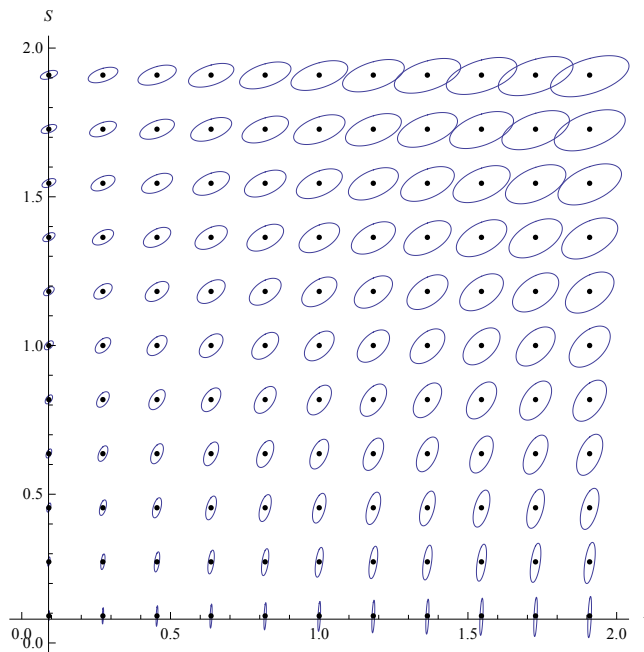


Figure 4: A plot of the Heston model (14) with parameter values  $\xi = 1$ ,  $\theta = 0.4$ ,  $\kappa = 1$ ,  $\mu = 0.1$ ,  $\rho = 0.5$  and where we have plotted the image of the epsilon balls for  $\epsilon = 0.05$

## 4 Itô & Stratonovich as different coordinates

For simplicity, let us assume in this section that the driver is one dimensional. Thus to define an SDE on a manifold, one must choose a 2-jet of a curve at each point of the manifold. One way to specify a  $k$ -jet of a curve at every point in an a neighbourhood is to first choose a chart for the neighbourhood and then consider curves of the form:

$$\gamma_x(t) = x + \sum_{i=1}^k a_i(x)t^i \quad (15)$$

where  $a_i : \mathbb{R}^n \rightarrow \mathbb{R}^n$ . As we have already seen in Lemma 1, these coefficient functions  $a_i$  depend upon the choice of chart in a relatively complex way. For example for 2-jets the coefficient functions are not vectors but instead transform according to Itô's lemma. We will call this the *standard representation* for a family of  $k$ -jets.

An alternative way to specify the  $k$ -jet of a curve at every point is to choose  $k$  vector fields  $A_1, \dots, A_k$  on the manifold. One can then define  $\Phi_{A_i}^t$  to be the vector flow associated with the vector field  $A_i$ . This allows one to define curves

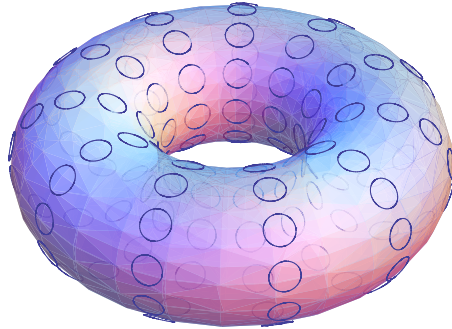


Figure 5: Plot of the SDE defining the Riemannian Brownian motion on the torus corresponding to the induced metric on the torus

at each point  $x$  as follows:

$$\gamma_x(t) = \Phi_{A_k}^{t^k} (\Phi_{A_{k-1}}^{t^{k-1}} (\dots (\Phi_{A_1}^t(x)) \dots)) \quad (16)$$

where  $t^k$  denotes the  $k$ -th power of  $t$ . We will call this the *vector representation* for a family of  $k$ -jets. It is not immediately clear that all  $k$ -jets of curves can be written in this way. Let us prove this.

Suppose one chooses a chart and attempts to compute the relationship between the coefficients  $a_i$  in the standard representation and the components of the vector fields  $A_i$  in the vector representation. It is clear that the  $o(t)$  term  $a_1(x)$  will depend bijectively and linearly on  $A_1(x)$ . Thus there is a bijection between 1-jets written in the form (15) and 1-jets written in the form (16). The  $o(t^2)$  term will depend linearly upon  $A_2(x)$  together with a more complex term derived from  $A_1$  and its first derivative. Symbolically  $a_1(x) = \rho(A_2(x)) + f(A_1(x), (\nabla A_1)(x))$  where  $\rho$  is a linear bijection determined by the choice of chart. It follows that there is also a bijection between 2-jets written in the standard form and 2-jets written in the vector form. Inductively we have:

**Theorem 2.** *Smooth  $k$ -jets of a curves can be defined uniquely by a list of  $k$  vector fields  $X_1, \dots, X_k$  according to the formula (16)*

Notice that the vector representation specifically allows us to define a *family* of  $k$ -jets varying from point to point. In more technical language, the vector representation allows us to specify a section of the bundle of  $k$ -jets. If one only specifies vectors at a point rather than vector fields, one cannot define the vector flows and so equation (16) cannot be used to define a  $k$ -jet at the point. Thus

although there is no natural map from  $k$  vectors defined at a point to a  $k$ -jet of a curve, there is a natural map from  $k$  vector fields defined in a neighbourhood to a smoothly varying choice of  $k$ -jet at each point.

The standard and vector representations simply give us two different coordinate systems for the infinite dimensional space of families of  $k$ -jets.

When this general theory about  $k$ -jets is applied to stochastic differential equations one sees that two corresponding coordinate representations of a stochastic differential equation will emerge. Let us calculate in more detail correspondence between the two representations.

**Lemma 2.** *Suppose that a family of 2-jets of curves is given in the vector representation as*

$$\gamma_x(t) = \Phi_A^{t^2}(\Phi_B^t(x))$$

for vector fields  $A$  and  $B$ . Choose a coordinate chart and let  $A^i$ ,  $B^i$  be the components of the vector fields in this chart. Then the corresponding standard representation for the family of 2-jets is:

$$\gamma_x(t) = x + a(x)t^2 + b(x)t$$

with

$$\begin{aligned} a^i &= A^i + \frac{1}{2} \frac{\partial B^i}{\partial x^j} B^j \\ b^i &= B^i. \end{aligned}$$

*Proof.* By definition of the flow  $\Phi_B^t$ , its components  $(\Phi_B^t)^i$  satisfy:

$$\frac{\partial (\Phi_B^t(x))^i}{\partial t} = B^i(\Phi_B^t(x)) \quad (17)$$

Differentiating this we have:

$$\begin{aligned} \frac{\partial^2 (\Phi_B^t(x))^i}{\partial t^2} &= \frac{\partial B^i}{\partial x^j} \frac{\partial (\Phi_B^t)^j}{\partial t} \\ &= B^j \frac{\partial B^i}{\partial x^j}. \end{aligned} \quad (18)$$

We now compute the derivatives of  $\gamma_t(x)$ . We write  $(\Phi_A^{t^2})^i$  for the  $i$ -th component of the function  $\Phi_A^{t^2}$ .

$$\frac{\partial}{\partial t} ((\Phi_A^{t^2})^i(\Phi_B^t(x))) = 2t \frac{\partial (\Phi_A^{t^2})^i}{\partial t}(\Phi_B^t) + \frac{\partial (\Phi_A^{t^2})^i}{\partial x^j}(\Phi_B^t) \frac{\partial (\Phi_B^t)^j}{\partial t}$$

Differentiating this again one obtains:

$$\begin{aligned} \frac{\partial^2}{\partial t^2} ((\Phi_A^{t^2})^i(\Phi_B^t(x))) &= 4t^2 \frac{\partial^2 (\Phi_A^{t^2})^i}{\partial t^2}(\Phi_B^t) + 2 \frac{\partial (\Phi_A^{t^2})^i}{\partial t}(\Phi_B^t) + 4t \frac{\partial^2 (\Phi_A^{t^2})^i}{\partial x^j \partial t}(\Phi_B^t) \frac{\partial (\Phi_B^t)^j}{\partial t} \\ &\quad + \frac{\partial^2 (\Phi_A^{t^2})^i}{\partial x^j \partial x^k}(\Phi_B^t) \frac{\partial (\Phi_B^t)^j}{\partial t} \frac{\partial (\Phi_B^t)^k}{\partial t} + \frac{\partial (\Phi_A^{t^2})^i}{\partial x^j} \frac{\partial \Phi_B^t}{\partial t^2} \end{aligned}$$

At time  $t = 0$  we have that  $\Phi_A^0$  is simply the identity. So its partial derivatives at time 0 are trivial to compute. Hence

$$\begin{aligned} \frac{\partial^2}{\partial t^2} ((\Phi_A^{t^2})^i (\Phi_B^t(x))) \Big|_{t=0} &= 2 \frac{\partial (\Phi_A^{t^2})^i}{\partial t} (\Phi_B^t) + \frac{\partial (\Phi_B^t)^i}{\partial t^2} \\ &= 2A^i + B^j \frac{\partial B^i}{\partial x^j} \end{aligned}$$

The last line follows from the definition of  $\Phi_A^t$  as the flow associated with the vector  $A$  together with equation (18). We can now write down the expression for  $a(x)$ . The expression for  $b(x)$  follows immediately from equation (17).  $\square$

As we have already discussed, the standard representation of a 2-jet corresponds to conventional *Itô calculus*. What we have just demonstrated is that the vector representation of a 2-jet corresponds to *Fisk–Stratonovich–McShane calculus* [8] [17] [21] (Stratonovich from now on). Moreover we have given a geometric interpretation of how the coordinate free notion of a 2-jet of a curve is related to the vector fields defining a Stratonovich SDE.

It is worth now discussing the different stochastic calculi in the light of the above result. Despite the initial seminal paper by Itô [13] in a Itô calculus context, where Itô’s formula is used to change coordinates for a SDE on a manifold, Stratonovich calculus has been the main calculus when interfacing stochastic analysis with differential geometry [6, 20]. We used Stratonovich calculus ourselves in our past works on stochastic differential geometry applications to signal processing [3], see also [4], [5]. Stratonovich calculus has become so dominant in stochastic differential geometry that some authors have even asserted that stochastic differential geometry *requires* the use of Stratonovich calculus. As Itô’s paper long ago demonstrated, this is not the case. Indeed under the formalism one can argue that it is still the Itô calculus that “does all the work” ([20], Chapter V.30, p. 184).

From the point of view of this paper, we consider these two calculi as being simply different coordinate systems for the same underlying coordinate-free stochastic differential equation. As such one should choose the most convenient coordinate system for the problem at hand. Stratonovich calculus has some clear advantages, most notably the transformation rule for vector fields is simpler than that for 2-jets written using the standard representation. Itô calculus also has some clear advantages, it has simpler probabilistic properties stemming from the fact that the Itô integral is non-anticipative and results in a martingale.

If one likes to think of differential geometry from an extrinsic perspective (i.e. if one doesn’t like to think in terms of charts, but instead in terms of manifolds embedded in  $\mathbb{R}^n$ ) then Stratonovich calculus may appear to be necessary since an SDE remains confined to a submanifold  $M$  almost surely if the  $A$  and  $B$  vector fields are tangent to the manifold. This means that it is easy to write down the Stratonovich SDE induced on a submanifold from a Stratonovich SDE on  $\mathbb{R}^n$ . However, this convenience is in no way fundamental. Indeed this phenomenon is simply a consequence of the fact that under these circumstances the curvature of the 2-jet of the curve follows the curvature of the manifold.

In general, since Stratonovich calculus and Itô calculus are just two coordinate systems one would expect to be able to work using either calculus interchangeably. The most important difference between Stratonovich calculus and Itô calculus arises during the modelling process. It is when choosing what equation to write down in the first place that the choice between the calculi is most telling. Note that the modelling process is not a strictly mathematical process: it relies upon the modellers intuition.

From a modelling point of view Itô calculus has a strong advantage for applications to subjects such as mathematical finance, where one considers decision makers who cannot use information about the future. The non-anticipative nature of the Itô integral will make it easier to write down models for such problems using Itô calculus. On the other hand in subjects such as physics or engineering conservation laws and time-symmetry may be paramount, in which case modelling with the Stratonovich calculus may be simpler.

## 5 Fan Diagrams

In this section we will discuss how statistical properties of stochastic differential equations can be read off from the coefficients of the SDE and how these properties can be illustrated using *fan diagrams*.

A *fan diagram* is a standard tool in econometrics for illustrating the predictions of a model. In Figure 6 we have plotted a fan diagram for a stock price modelled by geometric Brownian motion. The negative times in the plot show historical values for the stock price. For positive times, we plot a single random realization of geometric Brownian motion together with two percentiles that indicate the range of values attained by other realizations. We have chosen to plot the percentiles  $\Phi(1) \approx 84\%$  and  $\Phi(-1) \approx 16\%$ .

Standard statistical properties of a distribution depend upon the coordinate system used for the distribution. For example the definition of the mean of a process in  $\mathbb{R}^n$  involves the vector space structure of  $\mathbb{R}^n$ . For this reason one would expect the trajectory of the mean of a process to depend upon the vector space structure. If one makes a non-linear transformation of  $\mathbb{R}^n$  the trajectory of the mean changes. Indeed Itô's lemma tells us that the trajectory does not even remain constant to first order under coordinate changes.

Another manifestation of the same phenomenon is the fact that given an  $\mathbb{R}$  valued random variable  $X$  and a non-linear function  $f$ , then  $\mathbb{E}(f(X)) \neq f(\mathbb{E}(X))$ . Again this arises because the definition of mean depends upon the vector space structure and  $f$  may not respect this.

However, the definition of the  $\alpha$ -percentile depends only upon the ordering of  $\mathbb{R}$  and not its vector space structure. As a result, for continuous monotonic  $f$  and  $X$  with connected state space, the median of  $f(X)$  is equal to  $f$  applied to the median of  $X$ . If  $f$  is strictly increasing, the analogous result holds for the  $\alpha$  percentile. If  $f$  is decreasing, the  $\alpha$  percentile of  $f(X)$  is given by  $f$  applied to the  $1 - \alpha$  percentile of  $X$ .

This has the implication that the trajectory of the  $\alpha$ -percentile of an  $\mathbb{R}$  valued

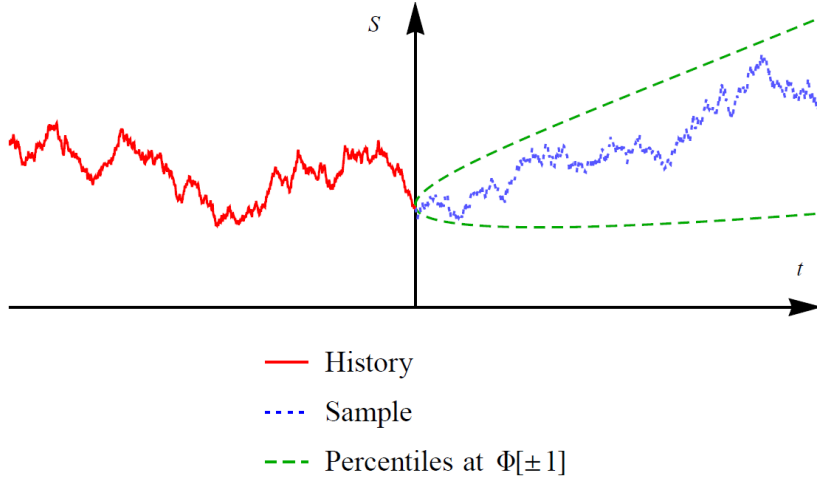


Figure 6: A fan diagram for a stock price,  $S$  modelled using geometric Brownian motion

stochastic process is invariant under smooth monotonic coordinate changes of  $\mathbb{R}$ . In other words, percentiles have a coordinate free interpretation. The mean does not. This raises the question of how the trajectories of the percentiles can be related to the coefficients of the stochastic differential equation. We will now calculate this relationship.

First we note that all smooth one dimensional Riemannian manifolds are isomorphic. When interpreted in terms of SDEs, this tells us that for any one dimensional SDE with non-vanishing volatility term:

$$dX_t = a(X_t, t) dt + b(X_t, t) dW_t, \quad X_0 = x_0 \quad (19)$$

we can find a coordinate system with respect to which the volatility term is equal to one. Such a transformation is known as a Lamperti transformation (see for example [18]) and is given by  $Z_t = \phi(t, X_t)$  where  $\phi(t, x)$  is a primitive integral of  $1/b(x, t)$  with respect to  $x$ . Let

$$dZ_t = \alpha(Z_t, t) dt + dW_t, \quad Z_0 = z_0 = \phi(0, x_0)$$

be the transformed equation. Since one dimensional Riemannian manifolds are translation invariant, we have a gauge freedom in defining a Lamperti transformation determined by the base-point of the isomorphism. Define a path  $z^0(t)$  by the ordinary differential equation:

$$\frac{dz^0}{dt} = \alpha(z^0(t), t), \quad z^0(0) = z_0.$$

If we set  $Y_t = Z_t - z^0(t)$  then  $Y$  follows the SDE

$$dY_t = \bar{a}(Y_t, t) dt + dW_t, \quad \bar{a}(y, t) = \alpha(y + z^0(t), t) - \alpha(z^0(t), t), \quad Y_0 = 0, \quad (20)$$

and moreover the drift of the  $Y$  SDE vanishes at 0 for all  $t$ ,  $\bar{a}(0, t) = 0$ .

Summing up, if  $b(x, t)$  is nowhere vanishing, there is a unique time dependent transformation that maps the original SDE (19) for  $X$  into a SDE with constant diffusion coefficient, zero initial condition and zero drift at zero. Actually, sufficient conditions for the Lamperti transformed SDE (20) to have a unique strong solutions are more stringent. For example, in the autonomous case  $a(x, t) = a(x)$  and  $b(x, t) = b(x)$  one may need  $a$  and  $b$  bounded from below and above, with  $b$  and its bounds strictly positive, with  $a \in C^1$  and  $b \in C^2$ . We will assume in the following that sufficient conditions for the solution of the Lamperti transformed SDE to exist unique hold.

Thus given a one dimensional SDE with non-vanishing volatility we can always make a transformation such that (subject to bounds) the following proposition applies (we denote  $\bar{a}$  by  $a$  for simplicity).

**Proposition 1.** *Let  $a(x, t)$  be a bounded smooth function on  $\mathbb{R} \times [0, +\infty)$  with  $a(0, t) = 0$ . Define the operators  $L$  and its adjoint  $L^*$  as*

$$Lp = \frac{1}{2} \frac{\partial^2 p}{\partial x^2} + a(x, t) \frac{\partial p}{\partial x} - \frac{\partial p}{\partial t}, \quad (21)$$

$$L^*p = \frac{1}{2} \frac{\partial^2 p}{\partial x^2} - \frac{\partial(a(x, t)p)}{\partial x} - \frac{\partial p}{\partial t}. \quad (22)$$

Assume further that  $a(x, t)$  has additional regularity required to ensure existence and uniqueness of a fundamental solution for the PDEs  $Lp = 0$  and  $L^*p = 0$ . Let  $\Gamma(x, t; \xi, \tau)$  be the fundamental solution of  $Lp = 0$ . Then for  $\lambda \in (0, 1)$  and a fixed terminal time  $T$ ,  $\Gamma$  satisfies:

$$\Gamma(x, t; 0, 0) = \frac{1}{\sqrt{2\pi t}} \exp\left(-\frac{x^2}{2t}\right) + O\left(\frac{t+x^2}{\sqrt{t}} \exp\left(-\frac{\lambda x^2}{2t}\right)\right)$$

on  $\mathbb{R} \times [0, T]$ , and the fundamental solution of  $L^*p = 0$  satisfies

$$\Gamma^*(0, 0; x, t) = \Gamma(x, t; 0, 0)$$

(see [9] for the definition of a fundamental solution.)

*Proof.* Equation  $L^*p = 0$  as the evolution for the density of a solution of a SDE is studied for example in Friedman's SDE book [10], see Eq. 5.28 in Chapter 6: by Theorem 4.7 in Ch 6 the fundamental solution of  $L^*p = 0$  is the same as the fundamental solution of  $Lp = 0$ . We will thus focus on  $Lp = 0$ , for which one can refer to Ch 1 Section 6 of Friedman's parabolic PDEs book [9]. When  $a$  is identically zero, the fundamental solution of  $Lp = 0$  in (21) is given by:

$$Z(x, t; \xi, \tau) = \frac{1}{\sqrt{2\pi(t-\tau)}} \exp\left(-\frac{(x-\xi)^2}{2(t-\tau)}\right).$$

By ([9] Ch 1, Theorem 10, p. 23), the fundamental solution of (21) is given by:

$$\Gamma(x, t; \xi, \tau) = Z(x, t; \xi, \tau) + \int_{\tau}^t \int_{\mathbb{R}} Z(x, t; \eta, \sigma) \Phi(\eta, \sigma; \xi, \tau) d\eta d\sigma \quad (23)$$

where

$$\Phi(x, t; \xi, \tau) = \sum_{i=1}^{\infty} \Phi_i(x, t; \xi, \tau)$$

where we define  $\Phi_1 = LZ$  and for  $i \geq 1$  we define

$$\Phi_{i+1}(x, t; \xi, \tau) = \int_{\tau}^t \int_{\mathbb{R}} L Z(x, t; y, \sigma) \Phi_i(y, \sigma, \xi, \tau) dy d\sigma.$$

Let us define:

$$\Gamma_i(x, t; \xi, \tau) := \int_{\tau}^t \int_{\mathbb{R}} Z(x, t; \eta, \theta) \Phi_i(\eta, \theta; \xi, \tau) d\eta d\theta.$$

First we bound  $\Gamma_1$ .

$$\begin{aligned} \Gamma_1(x, t; \xi, \tau) &= \int_{\tau}^t \int_{\mathbb{R}} Z(x, t; \eta, \sigma) LZ(\eta, \sigma; \xi, \tau) d\eta d\sigma \\ &= \int_{\tau}^t \int_{\mathbb{R}} Z(x, t; \eta, \sigma) a(\eta, \sigma) \frac{\partial}{\partial \eta} Z(\eta, \sigma; \xi, \tau) d\eta d\sigma. \end{aligned}$$

The final line follows because  $Z$  is the fundamental solution of (21) when  $a$  is equal to zero and so the parts of  $\Gamma_1$  that don't involve  $a$  vanish. Our assumptions ensuring Lipschitz continuity of  $a(x, t)$  uniformly in  $t$  and the fact that  $a(0, t) = 0$  for all  $t$  (see (20)) tell us that there is some constant with  $|a(x, t)| < C|x|$  for all  $x$  and  $t \in [0, T]$ . So

$$\begin{aligned} \left| a(\eta, \sigma) \frac{\partial}{\partial \eta} Z(\eta, \sigma; 0, 0) \right| &= \left| -\frac{1}{\sqrt{2\pi\sigma}} a(\eta, \sigma) \eta \exp\left(-\frac{\eta^2}{2\sigma}\right) \right| \\ &< \frac{C}{\sqrt{2\pi\sigma}} \eta^2 \exp\left(-\frac{\eta^2}{2\sigma}\right) \end{aligned}$$

We deduce that

$$\begin{aligned} |\Gamma_1(x, t; 0, 0)| &\leq C \int_0^t \int_{\mathbb{R}} Z(x, t; \eta, \sigma) \eta^2 \frac{1}{\sqrt{2\pi\sigma}} \exp\left(-\frac{\eta^2}{2\sigma}\right) d\eta d\sigma \\ &= C \frac{e^{-\frac{x^2}{2t}} (t + x^2)}{2\sqrt{2\pi t}} \end{aligned}$$

The final step follows simply by the routine evaluation of the integral. To do this we use estimates which were used in [9] to prove that our expression for  $\Gamma$  exists and is a fundamental solution. First, we have for any  $\lambda \in (0, 1)$  that:

$$|Z(x, t, \xi, \tau)| \leq \frac{1}{(t - \tau)^{\frac{1}{2}}} \exp\left(-\frac{\lambda|x - \xi|^2}{2(t - \tau)}\right).$$

From ([9] Ch 1, 4.14, p. 16) we have that there exist positive constants  $H$  and  $H_0$  such that for all  $\lambda \in (0, 1)$  and  $m \geq 2$ :

$$|\Phi_m(x, t; \xi, \tau)| \leq \frac{H_0 H^m}{\Gamma_E(m)} (t - \tau)^{m - \frac{3}{2}} \exp\left(-\frac{\lambda|x - \xi|^2}{2(t - \tau)}\right)$$

where  $\Gamma_E$  is the gamma function. From ([9] Ch 1, Lemma 3 p. 15) we have that if  $r < \frac{3}{2}$  and  $s < \frac{3}{2}$  then:

$$\begin{aligned} & \int_{\sigma}^{\tau} \int_{\mathbb{R}} (t-\tau)^{-r} \exp\left(-\frac{h(x-\xi)^2}{2(t-\tau)}\right) (\tau-\sigma)^{-s} \exp\left(-\frac{h(x-\xi)^2}{2(t-\sigma)}\right) d\xi d\sigma \\ &= \sqrt{\frac{2\pi}{h}} B\left(\frac{3}{2}-r, \frac{3}{2}-s\right) (t-\sigma)^{\frac{3}{2}-r-s} \exp\left(-\frac{h(x-y)^2}{2(t-\sigma)}\right) \end{aligned}$$

where  $B$  is the beta function. Taking  $r = 1/2$  and  $s = \frac{3}{2} - m$  we obtain the estimate:

$$\begin{aligned} |\Gamma_m(x, t; \xi, \tau)| &\leq \frac{H_0 H^m}{\Gamma_E(m)} \sqrt{\frac{2\pi}{\lambda}} B(1, m) (t-\tau)^{-\frac{1}{2}+m} \exp\left(-\frac{\lambda(x-\xi)^2}{2(t-\tau)}\right) \\ &= \frac{H_0 H^m}{m!} \sqrt{\frac{2\pi}{\lambda}} (t-\tau)^{-\frac{1}{2}+m} \exp\left(-\frac{\lambda(x-\xi)^2}{2(t-\tau)}\right) \end{aligned}$$

So

$$\begin{aligned} \sum_{k=2}^{\infty} |\Gamma_m(x, t; 0, 0)| &\leq \sum_{m=2}^{\infty} H_0 \frac{H^m}{m!} t^{-\frac{1}{2}+m} \exp\left(-\frac{\lambda x^2}{2t}\right) \\ &= \sqrt{\frac{2\pi}{\lambda}} H_0 H^2 \exp(Ht) (t)^{3/2} \exp\left(-\frac{\lambda x^2}{2t}\right) \end{aligned}$$

The result follows if we conclude by invoking Theorem 15, Ch 1, p. 28 of [9], or Theorem 4.7 in Ch 6 of [10].  $\square$

**Theorem 3.** *For sufficiently small  $t$ , the  $\alpha$ -th percentile of the solutions to (19) is given by:*

$$x_0 + b_0 \sqrt{t} \Phi^{-1}(\alpha) + (a_0 - b_0 b'_0) (1 - \Phi^{-1}(\alpha)^2) t + O(t^{3/2})$$

*so long as the coefficients of (19) are smooth, the diffusion coefficient  $b$  never vanishes, and sufficient conditions for the Lamperti transformed SDE and for  $L^*p = 0$  to have a unique regular solution hold. In this formula  $a_0$  and  $b_0$  denote the values of  $a(x_0, 0)$  and  $b(x_0, 0)$  respectively. In particular, the median process is a straight line up to  $O(t^{\frac{3}{2}})$  with tangent given by the drift of the Stratonovich version of the SDE (19). The  $\Phi(1)$  and  $\Phi(-1)$  percentiles correspond up to  $O(t^{\frac{3}{2}})$  to the curves  $\gamma_{X_0}(\pm\sqrt{t})$  where  $\gamma_{X_0}$  is any representative of the 2-jet that defines the SDE in Itô form.*

*Proof.* We first apply a Lamperti transformation so that the conditions of Proposition 1 apply. Let write  $y$  for the coordinates after applying the Lamperti transformation and let us write  $\rho$  for the 1-form representing the probability density. By Proposition 1

$$\rho = \left[ \frac{1}{\sqrt{2\pi t}} \exp\left(-\frac{y^2}{2t}\right) + O\left(\frac{t+y^2}{\sqrt{t}} \exp\left(-\frac{\lambda y^2}{2t}\right)\right) \right] dy$$

We introduce a new coordinate  $z = \frac{y}{\sqrt{t}}$  so that the density can be written:

$$\rho = \left[ \frac{1}{\sqrt{2\pi}} \exp\left(-\frac{z^2}{2}\right) + O\left(t(1+z^2) \exp\left(-\frac{\lambda z^2}{2}\right)\right) \right] dz$$

Integrating this, we see that for sufficiently small  $\epsilon$  we have a uniform estimate:

$$\int_{-\infty}^{\Phi^{-1}(\alpha+\epsilon)} \rho = \alpha + \epsilon + O(t).$$

It follows that the  $\alpha$ -th percentile in  $z$  coordinates is  $\Phi^{-1}(\alpha) + O(t)$ . Hence in  $y$  coordinates it is  $\phi^{-1}(\alpha)\sqrt{t} + O(t^{3/2})$

Let  $g$  denote the inverse of the Lamperti transformation that we have taken. Let us write the Taylor series expansion for  $g$  around  $(0,0)$  as:

$$g(y, t) = x_0 + g_y y + \frac{1}{2} g_{yy} y^2 + g_t t + O(y^2 + t)$$

By construction the SDE in  $y$  coordinates is of the form:

$$dY_t = \bar{a} dt + dW_t$$

with  $\bar{a}(0, t) = 0$ . When we apply  $g$  to this equation we will get equation (19). Using Itô's lemma we deduce that:

$$\begin{aligned} b &= g_y \\ a_0 &= g_t + \frac{1}{2} g_{yy} \end{aligned}$$

The first of these equations holds everywhere, the second uses the vanishing of  $\bar{a}$  at 0. To avoid notational ambiguity in partial differentiation, we will temporarily write  $s$  for the time coordinate when paired with  $x$  and  $t$  for the time coordinate when paired with  $y$ . Thus we are making the coordinate transformation:

$$\begin{aligned} x &= g(y, t) \\ s &= t \end{aligned}$$

We then have that:

$$\begin{aligned} \frac{\partial b}{\partial x} &= \frac{\partial b}{\partial y} \frac{\partial y}{\partial x} + \frac{\partial b}{\partial s} \frac{\partial s}{\partial x} \\ &= g_{yy} \frac{1}{g_y} \end{aligned}$$

So we have that at 0:

$$\begin{aligned} g_y &= b_0 \\ g_{yy} &= b_0 b'_0 \\ g_t &= \left( a_0 - \frac{1}{2} b_0 b'_0 \right) \end{aligned}$$

Putting these formulae together with our power series expansion for the percentile in  $y$  coordinates into the Taylor series expansion for  $g$  gives the desired result.  $\square$

The theorem above has given us the median as a special case, and a link between the median and the Stratonovich version of the SDE. By contrast the mean process has tangent given by the drift of the Itô SDE as the Itô integral is a martingale.

For completeness, besides the mean and the median, we wish to consider the mode. We claim that under the same conditions as the theorem above, there are paths  $m^u(t)$  and  $m^l(t)$  both satisfying:

$$\begin{aligned} m^u &= x_0 + a(x_0, 0)t - \frac{3}{2}b(x_0, 0)b'(x_0, 0)t + O(t^{\frac{3}{2}}) \\ m^l &= x_0 + a(x_0, 0)t - \frac{3}{2}b(x_0, 0)b'(x_0, 0)t + O(t^{\frac{3}{2}}) \end{aligned}$$

such that for sufficiently small  $t$  there exists a mode lying in  $[m^l(t), m^u(t)]$ . This relationship between the mean, median and mode is approximately seen in many general probability distributions as was observed qualitatively by Pearson [19].

We can consider as an example the case of geometric Brownian motion, where  $a(t, x) = \mu x$  and  $b(t, x) = \sigma x$  with  $\mu$  and  $\sigma$  deterministic constants,  $\sigma > 0$ . For this process the mean is easily computed from its lognormal distribution as  $x_0 \exp(\mu t)$ . To compute the median, we use Itô's formula and write the SDE for the logarithm, which is related to the Lamperti transform for this specific process,

$$d \ln X_t = (\mu - \sigma^2/2)dt + \sigma dW_t, \ln(x_0).$$

Now this is a Gaussian process, so that its median is equal to its mean. This is easily calculated as  $\ln x_0 + (\mu - \sigma^2/2)t$ . Since the median transforms with increasing transformations, the median of  $X$  is just the inverse of the Lamperti transform of the median of  $\ln X_t$ , leading to the exponential  $x_0 \exp((\mu - \sigma^2/2)t)$ . Finally, for the lognormal distribution we know the mode to be  $x_0 \exp((\mu - 3\sigma^2/2)t)$ . Concluding, mode range, median and mean for the geometric Brownian motion are sorted in increasing order and are given respectively by

$$x_0 \exp((\mu - 3\sigma^2/2)t), \quad x_0 \exp((\mu - \sigma^2/2)t), \quad x_0 \exp(\mu t).$$

A first order expansion of the exponentials for small  $t$  would give us formulas consistent with our general result.

The geometric Brownian motion is a special case of our more general result. This result gives an alternative way of plotting the two jet that defines a one dimensional stochastic differential equation - at each point  $x \in \mathbb{R}$  one plots the curve  $(t, \gamma_x(\pm\sqrt{t}))$ . Such a plot is shown for the visually convenient geometric Brownian motion with vanishing drift  $\mu = 0$  in the left hand panel of Figure 7. One interprets this diagram as an infinitesimal fan-diagram showing the  $\Phi(1)$  and  $\Phi(-1)$  percentiles.

In the right hand panel of Figure 7 we show how this plot transforms when one sends  $(t, S_t)$  to  $(t, \log(S_t))$ . This is illustrated with solid lines. We also use dashed lines to plot the corresponding diagram for the equation arising from Itô's lemma:

$$d(\log(S_t)) = -\frac{1}{2}\sigma^2 dt + \sigma dW_t. \quad (24)$$

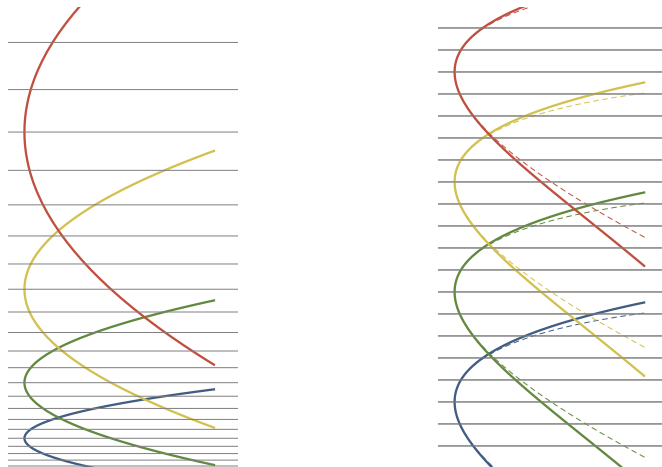


Figure 7: A fan diagram of Geometric Brownian motion (left). The result of applying  $(x, y) \rightarrow (x, \log y)$  to this fan diagram (right, solid line). A fan diagram of equation (24), the Brownian motion with drift associated with the  $\log S$  process (right, dashed line).

As predicted by our discussion so far, if one applies the logarithm to the vertical axis of the fan diagram for geometric Brownian motion one will approximately obtain the fan diagram for the equation (24). In the parlance of the geometry of curves, the dashed line is the *osculating curve* for the solid line in the family of fan diagrams of Brownian motions with drift.

It is interesting to notice that one can clearly see the drift term in the right hand side of Figure 7. Notice also that this drift arises because the spacing between the grid lines on the left hand side of figure 7 increases as one moves up the page whereas the corresponding grid lines after transformation are evenly spaced. This can be interpreted as a visual demonstration that the Itô term in the transformation rule for SDEs is determined by the second derivative of the transformation.

## A Proof of convergence to classical Itô calculus

In this appendix we prove Theorem 1, stating convergence in  $L^2(\mathbb{P})$  of the 2-jet scheme to the classical Itô solution of the SDE. The techniques used to prove

almost-sure convergence of the classical Euler scheme ([11] for example) could be adapted to the 2-jet scheme.

*Proof.* We think of  $T$  as fixed and as  $N$  increases  $\mathcal{T}^N$  provides a finer discretization grid approximating  $[0, T]$ .

To remove clutter from our equations, during this proof we will adopt the following conventions.  $C$  is a constant, independent of  $N$  that may change from line to line. We drop the superscript  $N$  from terms such as  $X_t^N$ . Sums over Greek indices always range from 1 to  $d$ .  $i, j$  and  $k$  are always integers. Terms with integer time subscripts such as  $X_i$  are shorthand for  $X_{i\delta t}$ . Superscript  $T$ 's indicate the vector transpose rather than the terminal time.

Under our hypotheses, we know from [15], Theorem 10.2.2 p. 342 that the Euler scheme:

$$\bar{X}_{t+\epsilon} = \bar{X}_t + a(\bar{X}_t)\epsilon + \sum_{\alpha} b_{\alpha}(\bar{X}_t)(W_{t+\epsilon}^{\alpha} - W_t^{\alpha}) \text{ for } t \in \mathcal{T}^N, \epsilon \in [0, \delta t]$$

converges to the solution of the Itô SDE in that:

$$\sup_{t \in [0, T]} E \left\{ |\bar{X}_t - \tilde{X}_t|^2 \right\} \leq C \delta t .$$

Our formula for the scheme incorporates interpolation in-between time steps, but the crude scheme is obtained by applying only time steps of size  $\delta t$ .

Since

$$\begin{aligned} \sup_{t \in [0, T]} E \left\{ |X_t - \tilde{X}_t|^2 \right\} &\leq \sup_{t \in [0, T]} E \left\{ 2|X_t - \bar{X}_t|^2 + 2|\bar{X}_t - \tilde{X}_t|^2 \right\} \\ &\leq 2 \sup_{t \in [0, T]} E \left\{ |X_t - \bar{X}_t|^2 \right\} + 2 \sup_{t \in [0, T]} E \left\{ |\bar{X}_t - \tilde{X}_t|^2 \right\} \end{aligned}$$

all we need to conclude with (10) is to show:

$$\sup_{t \in [0, T]} E \left\{ |X_t - \bar{X}_t|^2 \right\} \leq C \delta t .$$

Summing the differences of consecutive terms in the Euler scheme with time step  $\delta t$  we have:

$$\bar{X}_k = x_0 + \sum_{i=1}^k \left[ a(\bar{X}_{i-1})\delta t + \sum_{\alpha} b_{\alpha}(\bar{X}_{i-1})\delta W_{i-1}^{\alpha} \right]$$

where  $\delta W_k := W_{(k+1)\delta t} - W_{k\delta t}$ . Using the definition for  $a$  we can write this as:

$$\bar{X}_k = x_0 + \sum_{i=1}^k \left[ \sum_{\alpha, \beta} \tilde{a}_{\alpha, \beta}(\bar{X}_{i-1}) g_E^{\alpha \beta} \delta t + \sum_{\alpha} b_{\alpha}(\bar{X}_{i-1}) \delta W_{i-1}^{\alpha} \right] \quad (25)$$

where  $g_E$  is the metric tensor of the Euclidean metric and where we define

$$\tilde{a}_{\alpha,\beta}(x) := \frac{1}{2} \frac{\partial^2 \gamma_x}{\partial u^\alpha \partial u^\beta} \Big|_{u=0}, \quad \text{so that} \quad a = \sum_{\alpha,\beta} \tilde{a}_{\alpha,\beta} g^{\alpha,\beta}.$$

Note that we are not using the Einstein summation convention in this proof. Let us write the 2-jet scheme via its Taylor expansion as in (4), namely

$$X_k = X_{k-1} + \sum_{\alpha,\beta} \tilde{a}_{\alpha,\beta}(X_{k-1}) \delta W_{k-1}^\alpha \delta W_{k-1}^\beta + \sum_{\alpha} b_\alpha(X_{k-1}) \delta W_{k-1}^\alpha + R_k. \quad (26)$$

This expression defines the remainder  $R_k$ . Note that the remainder depends also on  $N$  but our notation has suppressed this. Summing the differences of consecutive terms, and substituting in the definition of  $b$  we obtain:

$$X_k = x_0 + \sum_{i=1}^k \left[ \sum_{\alpha,\beta} \tilde{a}_{\alpha,\beta}(X_{i-1}) \delta W_{i-1}^\alpha \delta W_{i-1}^\beta + \sum_{\alpha} b_\alpha(X_{i-1}) \delta W_{i-1}^\alpha + R_i \right]. \quad (27)$$

Subtracting equation (25) from (27) we obtain:

$$X_k - \bar{X}_k = P_k + \sum_{\alpha} Q_k^\alpha + \sum_{\alpha,\beta} S_k^{\alpha,\beta}$$

where we define:

$$\begin{aligned} P_k &:= \sum_{i=1}^k R_i \\ Q_k^\alpha &:= \sum_{i=1}^k [b(X_{i-1}) - b(\bar{X}_{i-1})] \delta W_{i-1}^\alpha \\ S_k^{\alpha,\beta} &:= \sum_{i=1}^k [\tilde{a}_{\alpha,\beta}(X_{i-1}) \delta W_{i-1}^\alpha \delta W_{i-1}^\beta - \tilde{a}_{\alpha,\beta}(\bar{X}_{i-1}) g_E^{\alpha,\beta} \delta t] \end{aligned}$$

We have that:

$$E \{|X_k - \bar{X}_k|^2\} \leq C \left( E \{|P_k|^2\} + \sum_{\alpha} E \{|Q_k^\alpha|^2\} + \sum_{\alpha,\beta} E \{|S_k^{\alpha,\beta}|^2\} \right).$$

We now wish to obtain bounds for each expectation on the right in terms of  $\delta t$  and the function:

$$Z(t) = \sup_{0 \leq s \leq t} E \{|X_s - \bar{X}_s|^2\}.$$

Using our bound on the third derivatives of  $\gamma$ , we can bound the remainder terms  $R_i$  as follows:

$$|R_i| \leq C \left( \sum_{\alpha} |\delta W_{i-1}^\alpha| \right)^3.$$

Let us write:

$$M := E \left\{ \left( \sum_{\alpha} |\delta W_{i-1}^{\alpha}| \right)^6 \right\}.$$

We calculate that:

$$\begin{aligned} E(|P_k|^2) &= E \left\{ \left| \sum_i R_i \right|^2 \right\} \leq CN^2 M \\ &\leq C \left( \frac{T}{\delta t} \right)^2 (\delta t)^{\frac{6}{2}} \\ &\leq C \delta t. \end{aligned}$$

Next we have:

$$\begin{aligned} E \{ |Q_k^{\alpha}|^2 \} &\leq E \left\{ \left| \sum_{i=1}^k [b(X_{i-1}) - b(\bar{X}_{i-1})] \delta W_{i-1}^{\alpha} \right|^2 \right\} \\ &\leq CE \left\{ \left| \sum_{i=1}^k |X_{i-1} - \bar{X}_{i-1}| \delta W_{i-1}^{\alpha} \right|^2 \right\} \\ &= CE \left\{ \sum_{i=1}^k |X_{i-1} - \bar{X}_{i-1}|^2 \delta t \right\} \\ &\leq C \int_0^{k\delta t} Z(s) ds. \end{aligned}$$

The second line follows from the first by the Lipschitz condition on the derivatives. The third line follows by the discrete Itô isometry or the tower property of conditional expectation coupled with independence of Brownian increments.

To bound  $S^{\alpha,\beta}$  we write it as a sum of two components  $S^{\alpha,\beta,1}$  and  $S^{\alpha,\beta,2}$  defined as follows:

$$\begin{aligned} S_k^{\alpha,\beta,1} &:= \sum_{i=1}^k \tilde{a}_{\alpha,\beta}(\bar{X}_{i-1}) (\delta W_{i-1}^{\alpha} \delta W_{i-1}^{\beta} - g_E^{\alpha,\beta} \delta t) \\ S_k^{\alpha,\beta,2} &:= \sum_{i=1}^k [\tilde{a}_{\alpha,\beta}(X_{i-1}) - \tilde{a}_{\alpha,\beta}(\bar{X}_{i-1})] \delta W_{i-1}^{\alpha} \delta W_{i-1}^{\beta} \end{aligned}$$

By expanding the square term using the definition of  $S^{\alpha,\beta,1}$  we find:

$$\begin{aligned} E \{ |S_k^{\alpha,\beta,1}|^2 \} &= \\ \sum_{i=1}^k \sum_{j=1}^k E \{ &\tilde{a}_{\alpha,\beta}^T(\bar{X}_{i-1}) \tilde{a}_{\alpha,\beta}(\bar{X}_{j-1}) (\delta W_{i-1}^{\alpha} \delta W_{i-1}^{\beta} - g_E^{\alpha,\beta} \delta t) (\delta W_{j-1}^{\alpha} \delta W_{j-1}^{\beta} - g_E^{\alpha,\beta} \delta t) \} \end{aligned}$$

When  $i \neq j$  the terms on the right hand side vanish. This is because we may assume WLOG that  $j > i$  in which case the last factor of the  $(i, j)$ -th term,

$$\delta W_{j-1}^\alpha \delta W_{j-1}^\beta - g_E^{\alpha, \beta} \delta t$$

is independent of the rest of the term and has expectation 0. We now quote 10.2.14 p. 343 in [15] to show:

$$E \{ |\bar{X}_k|^2 \} \leq C. \quad (28)$$

We now compute:

$$\begin{aligned} E \left\{ |S_k^{\alpha, \beta, 1}|^2 \right\} &= \sum_{i=1}^k E \left\{ |\tilde{a}_{\alpha, \beta}(\bar{X}_{i-1})|^2 (\delta W_{i-1}^\alpha \delta W_{i-1}^\beta - g_E^{\alpha, \beta} \delta t)^2 \right\} \\ &\leq \sum_{i=1}^k E \left\{ |\tilde{a}_{\alpha, \beta}(\bar{X}_{i-1})|^2 \right\} E \left\{ (\delta W_{i-1}^\alpha \delta W_{i-1}^\beta - g_E^{\alpha, \beta} \delta t)^2 \right\} \\ &\leq \sum_{i=1}^k C(\delta t)^2 E \left\{ |\tilde{a}_{\alpha, \beta}(\bar{X}_{i-1})|^2 \right\} \\ &\leq \sum_{i=1}^k C(\delta t)^2 E \left\{ (1 + \bar{X}_{i-1}^2) \right\} \\ &\leq \sum_{i=1}^k C(\delta t)^2 \\ &\leq C\delta t \end{aligned}$$

The second line follows from independence of Brownian motion increments. The third from the second by the scaling properties of Brownian motion increments. The fourth from our growth bounds on the second derivatives. The fifth from the bound (28).

We now compute a bound for the  $S_k^{\alpha,\beta,2}$  term.

$$\begin{aligned}
E \left\{ |S_k^{\alpha,\beta,2}|^2 \right\} &\leq 2 \sum_{i=0}^{k-1} \sum_{j=0}^i E \left\{ |(\tilde{a}_{\alpha,\beta}(X_i) - \tilde{a}_{\alpha,\beta}(\bar{X}_i))^T (\tilde{a}_{\alpha,\beta}(X_j) - \tilde{a}_{\alpha,\beta}(\bar{X}_j))| \right. \\
&\quad \left. \times |\delta W_i^\alpha \delta W_i^\beta \delta W_j^\alpha \delta W_j^\beta| \right\} \\
&\leq C \sum_{i=0}^{k-1} \sum_{j=0}^i (E \left\{ |(\tilde{a}_{\alpha,\beta}(X_i) - \tilde{a}_{\alpha,\beta}(\bar{X}_i))^T (\tilde{a}_{\alpha,\beta}(X_j) - \tilde{a}_{\alpha,\beta}(\bar{X}_j))| \right\} \\
&\quad \times E \left\{ |\delta W_i^\alpha \delta W_i^\beta \delta W_j^\alpha \delta W_j^\beta| \right\}) \\
&\leq C(\delta t)^2 \sum_{i=0}^{k-1} \sum_{j=0}^i E \left\{ |(\tilde{a}_{\alpha,\beta}(X_i) - \tilde{a}_{\alpha,\beta}(\bar{X}_i))^T \right. \\
&\quad \left. \times (\tilde{a}_{\alpha,\beta}(X_j) - \tilde{a}_{\alpha,\beta}(\bar{X}_j))| \right\} \\
&\leq C(\delta t)^2 \sum_{i=0}^{k-1} \sum_{j=0}^i (E \left\{ |(\tilde{a}_{\alpha,\beta}(X_i) - \tilde{a}_{\alpha,\beta}(\bar{X}_i))|^2 \right\} \\
&\quad + E \left\{ |(\tilde{a}_{\alpha,\beta}(X_j) - \tilde{a}_{\alpha,\beta}(\bar{X}_j))|^2 \right\})
\end{aligned}$$

We have used independence of Brownian motion increments to get from the first line to the second. Next we have used the scaling behaviour of Brownian increments. Next we used Young's Inequality. Applying now the Lipschitz property of  $\tilde{a}_{\alpha,\beta}$  we find:

$$\begin{aligned}
E \left\{ |S_k^{\alpha,\beta,2}|^2 \right\} &\leq C(\delta t)^2 \sum_{i=0}^{k-1} \sum_{j=0}^i (E \left\{ |X_i - \bar{X}_i|^2 \right\} + E \left\{ |X_j - \bar{X}_j|^2 \right\}) \\
&\leq C\delta t \sum_{i=0}^{k-1} Z(i\delta t) \\
&\leq C \int_0^{k\delta t} Z(t) dt
\end{aligned}$$

where we took into account the fact that  $i \leq N = T/\delta t$ , so that  $i(\delta t)^2 \leq C\delta t$ . Putting together all our bounds we have:

$$Z(t) \leq C \left( \delta t + \int_0^t Z(s) ds \right).$$

So by the Groenwall inequality,  $Z(t) \leq C\delta t$ . □

## References

- [1] J. Armstrong and D. Brigo. Dimensionality reduction for SDEs with differential geometric projection methods. *Working paper, forthcoming on arxiv.org*.

- [2] John Armstrong and Damiano Brigo. Extrinsic projection of Itô SDEs on submanifolds with applications to non-linear filtering. *To appear in: Nielsen, F., Critchley, F., & Dodson, K. (Eds), Computational Information Geometry for Image and Signal Processing, Springer Verlag*, 2016.
- [3] John Armstrong and Damiano Brigo. Nonlinear filtering via stochastic PDE projection on mixture manifolds in  $L^2$  direct metric. *Mathematics of Control, Signals and Systems*, 28(1):1–33, 2016.
- [4] D Brigo, B Hanzon, and F LeGland. A differential geometric approach to nonlinear filtering: The projection filter. *IEEE Transactions on automatic control*, 43:247–252, 1998.
- [5] D. Brigo, B. Hanzon, and F. LeGland. Approximate nonlinear filtering by projection on exponential manifolds of densities. *Bernoulli*, 5(3):495–534, 06 1999.
- [6] D. Elworthy. Geometric aspects of diffusions on manifolds. In *École d’Été de Probabilités de Saint-Flour XV–XVII, 1985–87*, pages 277–425. Springer, 1988.
- [7] M. Emery. *Stochastic calculus in manifolds*. Springer-Verlag, Heidelberg, 1989.
- [8] D. Fisk. Quasi-martingales and stochastic integrals. *PhD Dissertation, Michigan State University, Department of Statistics*, 1963.
- [9] Avner Friedman. *Partial differential equations of parabolic type*. Prentice-Hall, reprinted in 2008 by Dover-Publications, Englewood Cliffs N.J, 1964.
- [10] Avner Friedman. *Stochastic differential equations and applications, vol. I and II*. Academic Press, reprinted by Dover Publications, New York, 1975.
- [11] I. Gyongy. A note on Eulers approximations. *Potential Analysis*, (8):205–216, 1998.
- [12] Steven L Heston. A closed-form solution for options with stochastic volatility with applications to bond and currency options. *Review of financial studies*, 6(2):327–343, 1993.
- [13] K. Itô. Stochastic differential equations in a differentiable manifold. *Nagoya Math. J.*, (1):35–47, 1950.
- [14] P. E. Kloeden and E. Platen. Higher-order implicit strong numerical schemes for stochastic differential equations. *Journal of statistical physics*, 66(1-2):283–314, 1992.
- [15] Peter E. Kloeden and Eckhard Platen. *Numerical solution of stochastic differential equations*. Applications of mathematics. Springer, Berlin, New York, Third printing, 1999.

- [16] S. Kobayashi and K. Nomizu. *Foundations of differential geometry*, volume 1. New York, 1963.
- [17] E.J. McShane. *Stochastic Calculus and Stochastic Models (2nd Ed.)*. Academic Press, New York, 1974.
- [18] G. A. Pavliotis. *Stochastic Processes and Applications: Diffusion Processes, the Fokker-Planck and Langevin Equations*. Springer, Heidelberg, 2014.
- [19] K. Pearson. Contributions to the mathematical theory of evolution. ii. skew variation in homogeneous material. *Philosophical Transactions of the Royal Society of London. A*, 186:343–414, 1895.
- [20] L. C. G. Rogers and D. Williams. *Diffusions, markov processes and martingales*, vol 2: Ito calculus, 1987.
- [21] R. L. Stratonovich. A new representation for stochastic integrals and equations. *SIAM Journal on Control*, 4(2):362–371, 1966.